Improved Oil-in-Place Estimates in Clay- and Pyrite-Bearing Shales*

Siddharth Misra[1] and Yifu Han[2]

Search and Discovery Article #41984 (2017)**
Posted January 30, 2017

*Adapted from oral presentation given at AAPG 2016 Eastern Section Meeting, Lexington, Kentucky, September 25-27, 2016

[1]University of Oklahoma, Norman, OK (misra@ou.edu)
[2]University of Oklahoma, Norman, OK

Abstract

Subsurface electromagnetic (EM) measurements, namely galvanic resistivity, EM induction, EM propagation, and dielectric dispersion, exhibit frequency dependence due to the interfacial polarization (IP) of clay minerals, clay-sized particles, and conductive minerals. Existing oil-in-place estimation methods based on subsurface EM measurements do not account for dielectric permittivity, dielectric dispersion, and dielectric permittivity anisotropy arising from the IP effects. The conventional interpretation methods generate inaccurate oil-in-place estimates in clay- and pyrite-bearing shales because they separately interpret the multi-frequency effective conductivity and permittivity using empirical models.

We introduce a new inversion-based method for accurate oil-in-place estimation in clay-and pyrite-bearing shales. The inversion algorithm is coupled with an electrochemical model that accounts for the frequency dispersion in effective conductivity and permittivity due to the above-mentioned IP effects. The proposed method jointly processes the multi-frequency effective conductivity and permittivity values computed from the subsurface EM measurements. The proposed method assumes negligible invasion, negligible borehole rugosity, and lateral and vertical homogeneity effects.

The successful application of the new interpretation method is documented with synthetic cases and field data. Water saturation estimates in shale formations obtained with the new interpretation method are compared to those obtained with conventional methods and laboratory measurements. Conventional interpretation of multi-frequency effective conductivity and permittivity well logs in a clay- and pyrite-rich shale formation generated water saturation estimates that varied up to 0.5 saturation units, as

a function of the operating frequency of the EM measurement, at each depth along the formation interval. A joint interpretation of multifrequency conductivity and permittivity is necessary to compute the oil-in-place estimates in such formations. Estimated values of water saturation, average grain size, and surface conductance of clays in that formation are in the range of 0.4 to 0.7, 0.5 micrometer to 5 micrometer, and 5×10^{-7} S to 9×10^{-7} S, respectively. The proposed method is a novel technique to integrate effective conductivity and permittivity at various frequencies. In doing so, the method generates frequency-independent oil-in-place estimates, prevents under-estimation of hydrocarbon saturation, and identifies by-passed zones in shales.

References Cited

Anderson, B., T. Barber, M. Lüling, J. Rasmus, P. Sen, J. Tabanou, and M. Haugland, 2007, Observations of Large Dielectric Effects on LWD Propagation-Resistivity Logs: SPWLA Annual Logging Symposium, Austin, Texas, June 3-6, Paper BB.

Misra, S., M.G. Lüling, J. Rasmus, D.M. Homan, and T.D. Barber, 2016, Dielectric Effects in Pyrite-Rich Clays on Multifrequency Induction Logs and Equivalent Laboratory Core Measurements: Society of Petrophysicists and Well-Log Analysts 57th Annual Logging Symposium, 25-29 June, Reykjavik, Iceland, SPWLA-2016-Z, 17 p.

Placencia-Gómez, E., L. Slater, D. Ntarlagiannis, and A. Binley, 2013, Laboratory SIP Signatures Associated with Oxidation of Disseminated Metal Sulfides: Journal of Contaminant Hydrology, v. 148, p. 25-38

Revil, A., 2012, Spectral Induced Polarization of Shaly Sands: Influence of the Electrical Double Layer: Water Resources Research, v. 48/2, W02517. doi:10.1029/2011WR011260

Revil, A., E. Atekwana, C. Zhang, A. Jardani, and S. Smith, 2012, A New Model for the Spectral Induced Polarization Signature of Bacterial Growth in Porous Media: Water Resources Research, 48, W09545. doi:10.1029/2012WR011965.

Wang, H., and A. Poppitt, 2013, The Broadband Electromagnetic Dispersion Formation Logging Data in a Gas Shale Formation - A Case Study: SPWLA 54th Annual Logging Symposium, New Orleans, Louisiana, June 22-26.

Improved Oil-in-Place Estimates in Clay- and Pyrite-Bearing Shales

Yifu Han and Siddharth Misra
University of Oklahoma

Presenter: Siddharth Misra

Outline

- Introduction and Motivation
- Multi-frequency conductivity-permittivity model
- Model predictions
- Multi-frequency conductivity-permittivity inversion
- Interpretation of Synthetic and Subsurface Data
- Conclusions

Introduction: Definition

Conductivity

$$\sigma$$

Frequency independent
No phase, Real Number

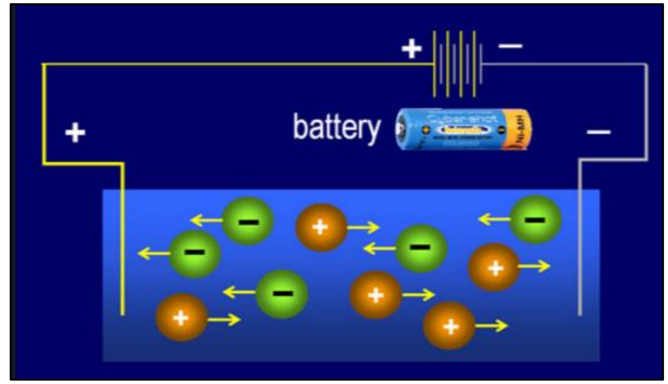

Flow

Permittivity

$$\varepsilon^*(\omega) = \varepsilon_r^*(\omega)\varepsilon_0$$

Complex relative permittivity

$$\varepsilon_r'(\omega) - i\varepsilon_r''(\omega)$$

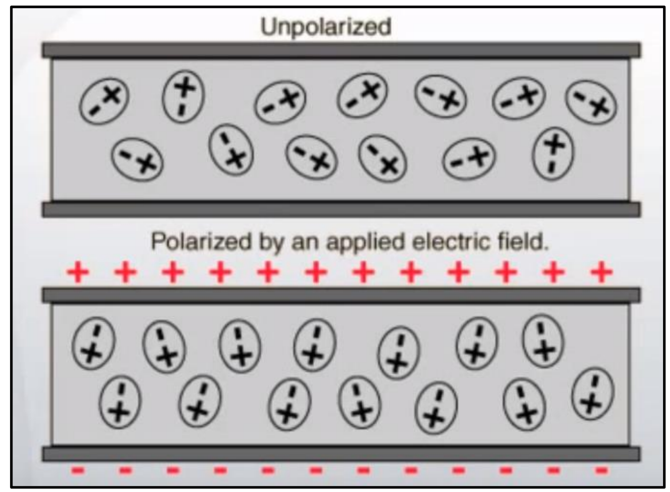

Storage

Conductivity measurement $(\sigma + \omega\varepsilon_r''\varepsilon_0) + i(\omega\varepsilon_r'\varepsilon_0)$

Relative permittivity measurement $\varepsilon_r' - i\left(\varepsilon_r'' + \frac{\sigma}{\omega\varepsilon_0}\right)$

Introduction: Definition

Polarization

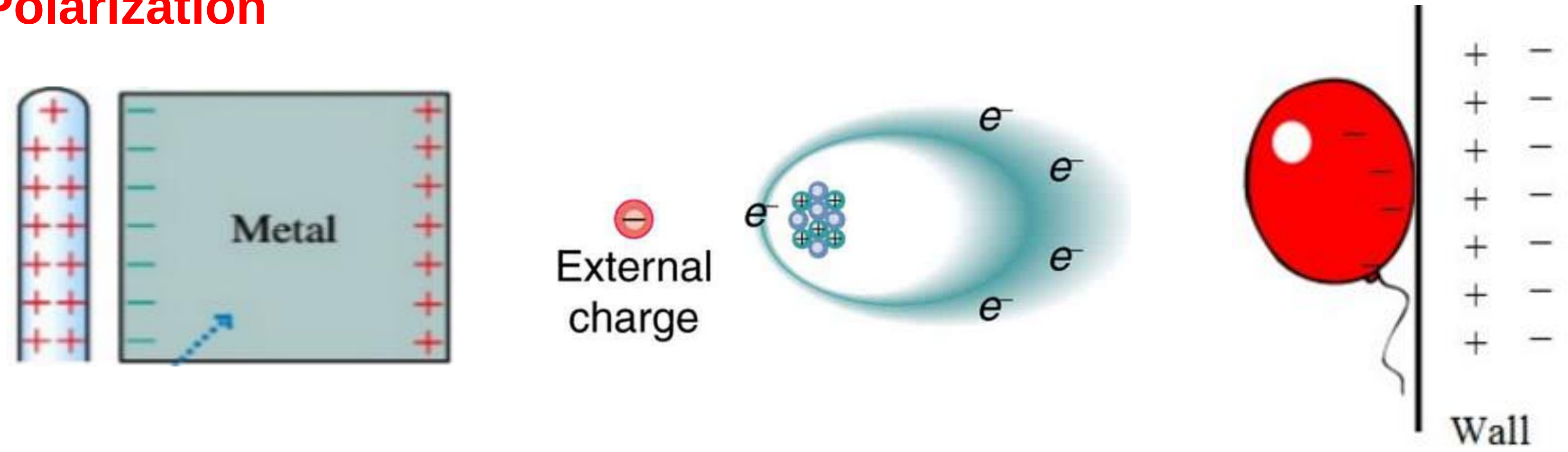

Dispersion

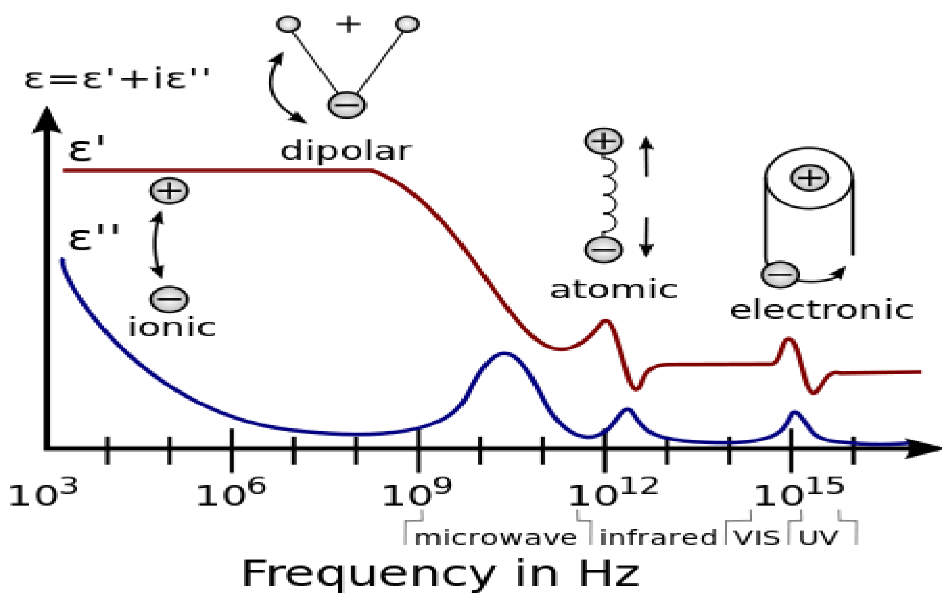

Introduction: Downhole EM Tools

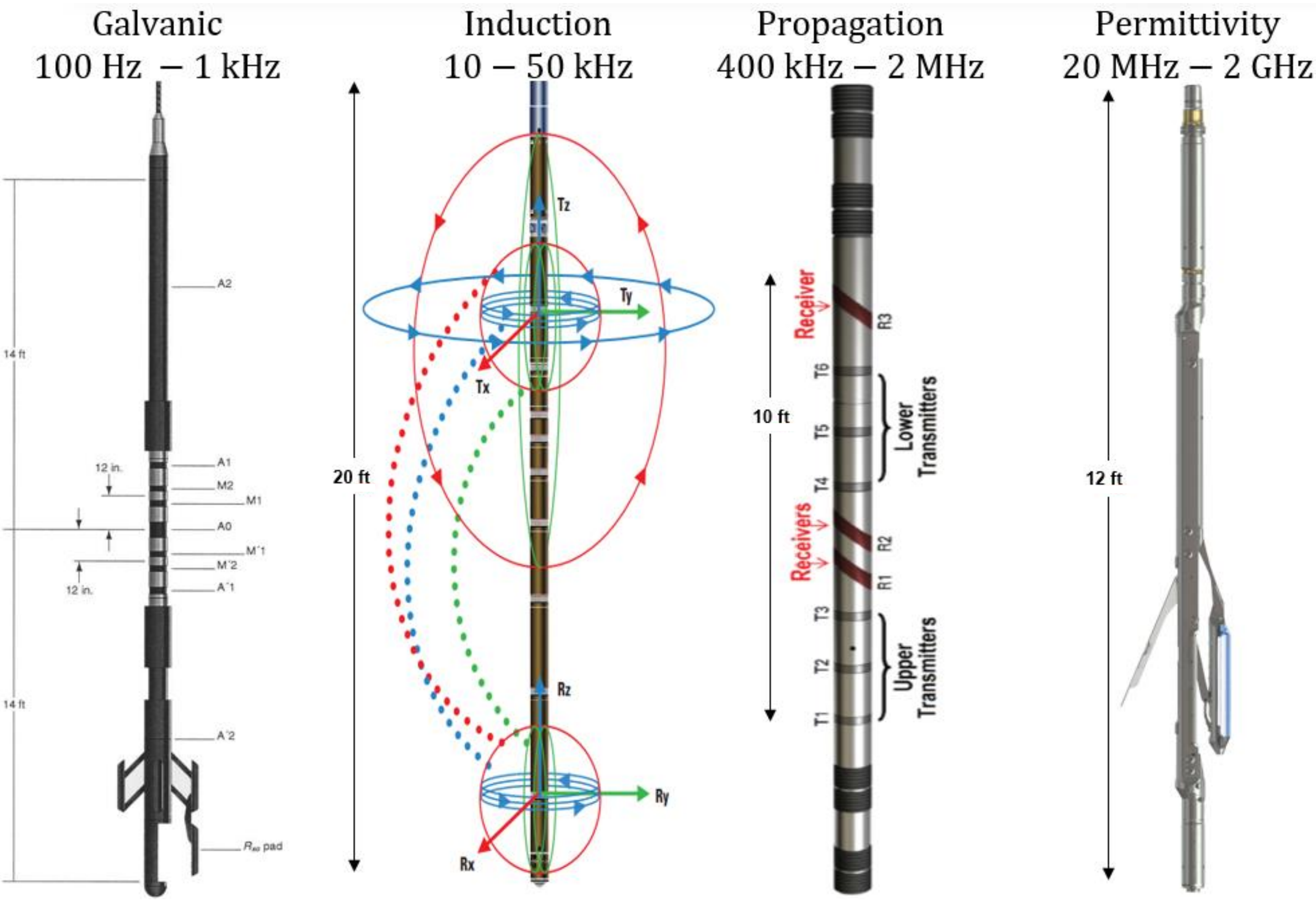

Introduction: Downhole EM Tools

Effects on EM log measurements

- Invasion
- Borehole
- Tool eccentricity
- Bed boundary
- Resistivity Anisotropy

- Interfacial polarization
- Frequency dispersion

Introduction: Pyrites and Clays

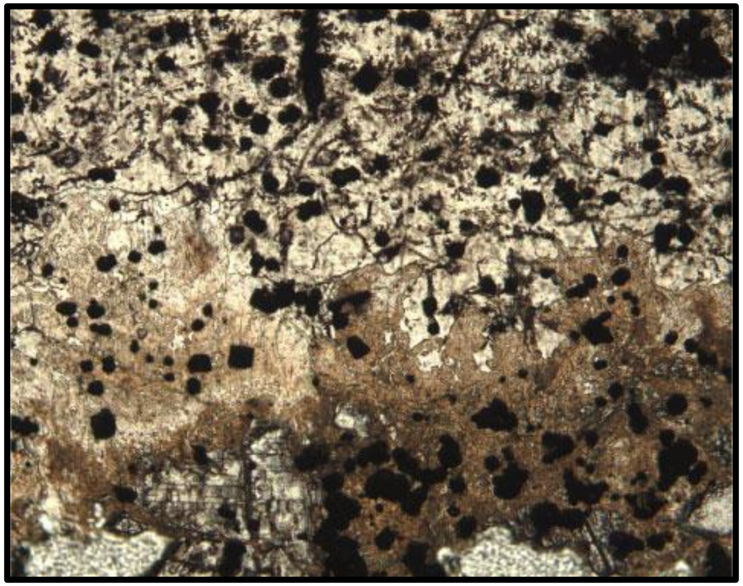

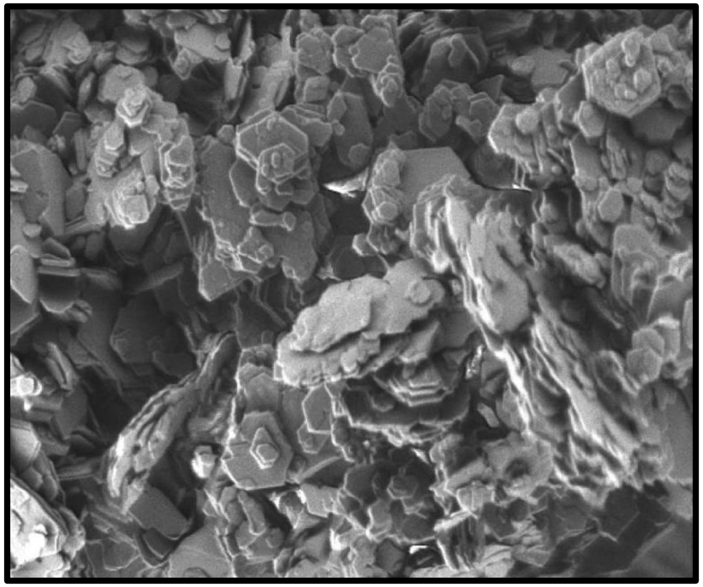

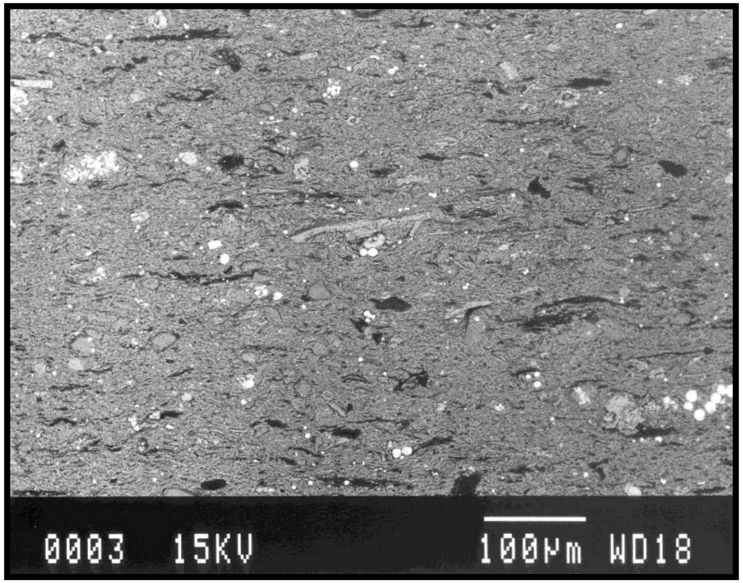

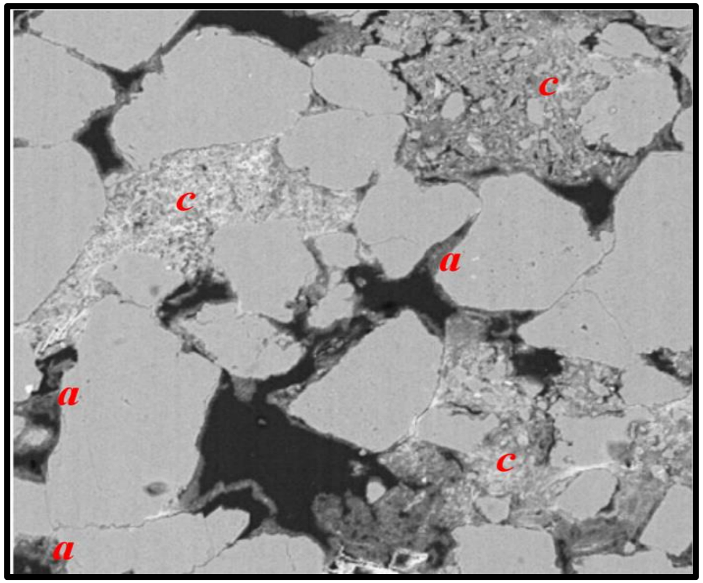

Introduction: Polarization

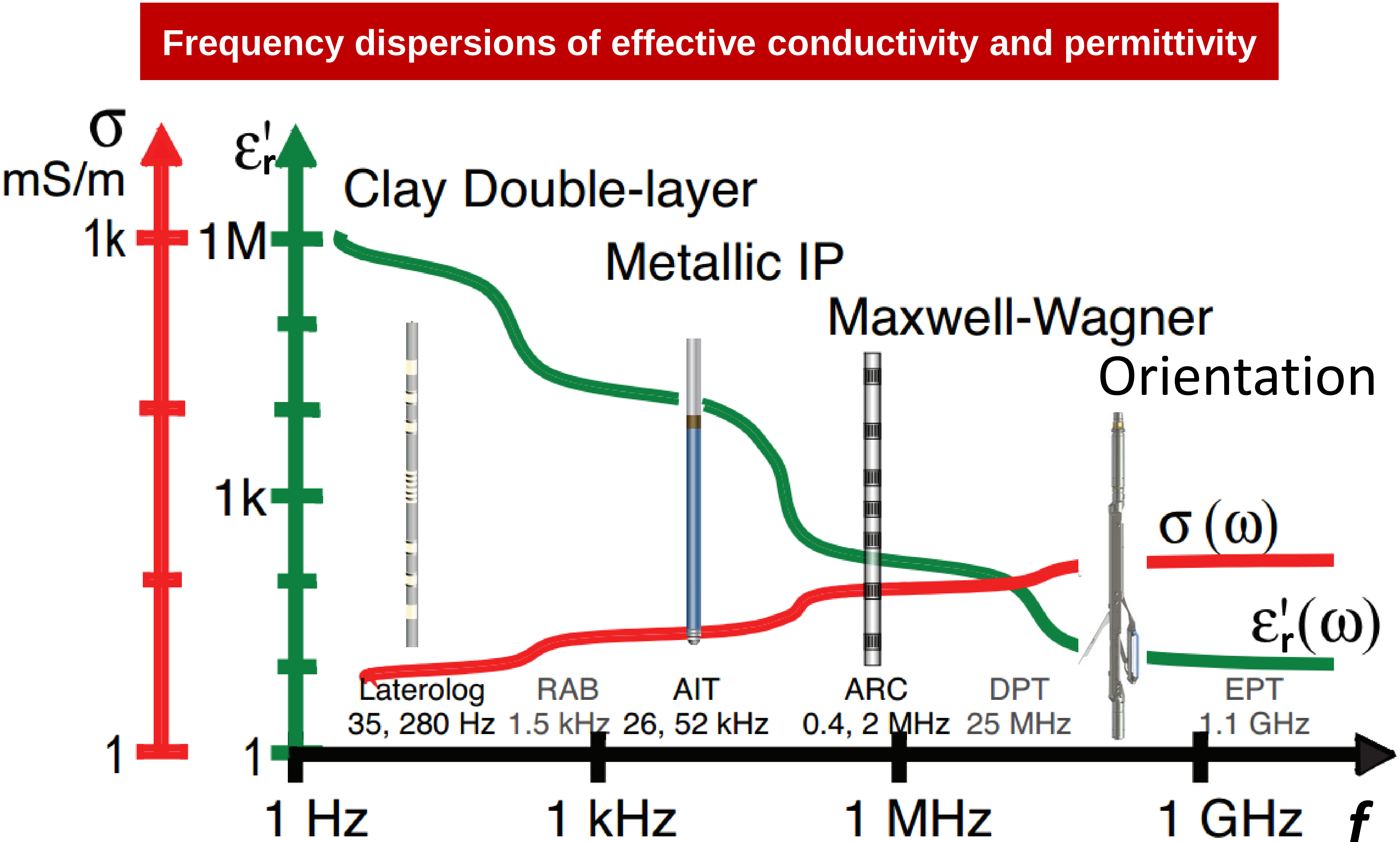

Anderson et al., 2007

Introduction: Polarization

Polarization of polar molecules – Orientation Polarization

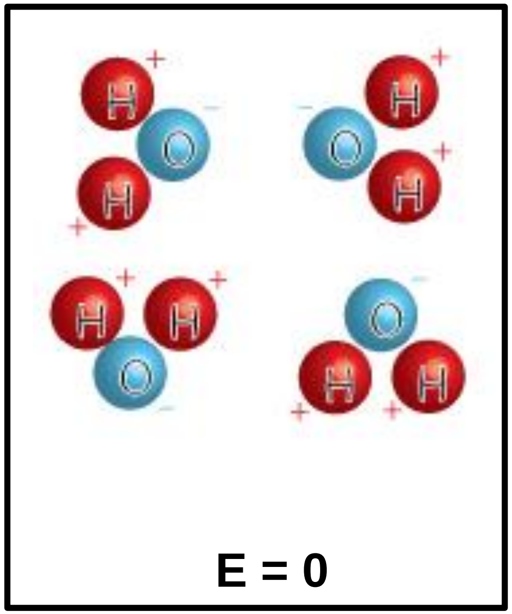

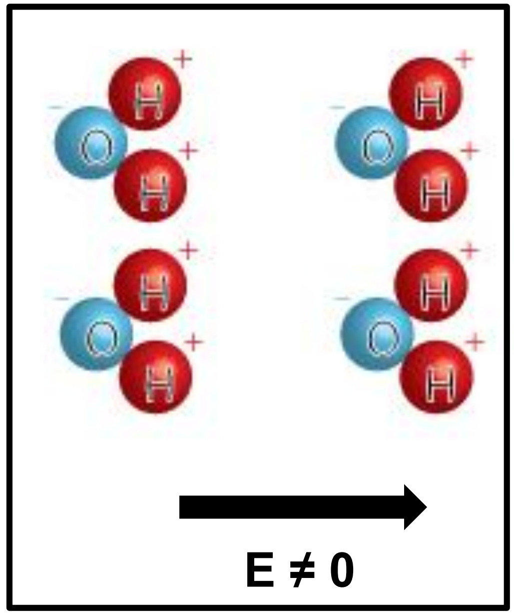

Orientation polarization is the only mechanism dominant around 1 GHz for hydrocarbon-bearing porous geomaterials

Introduction: Polarization

Interfacial polarization of conductive mineral grains – Metallic IP

Placencia-Gomez et al., 2013

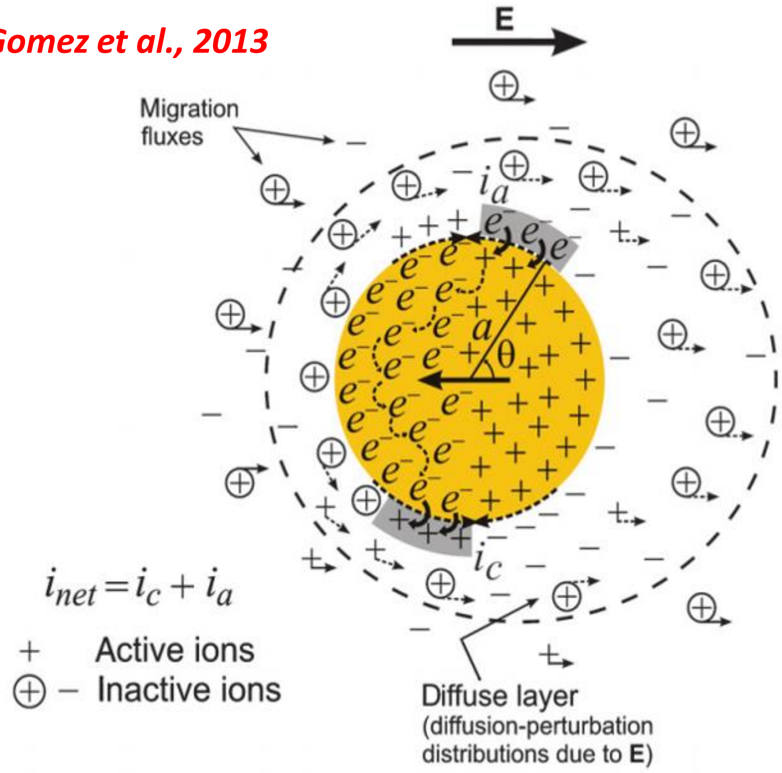

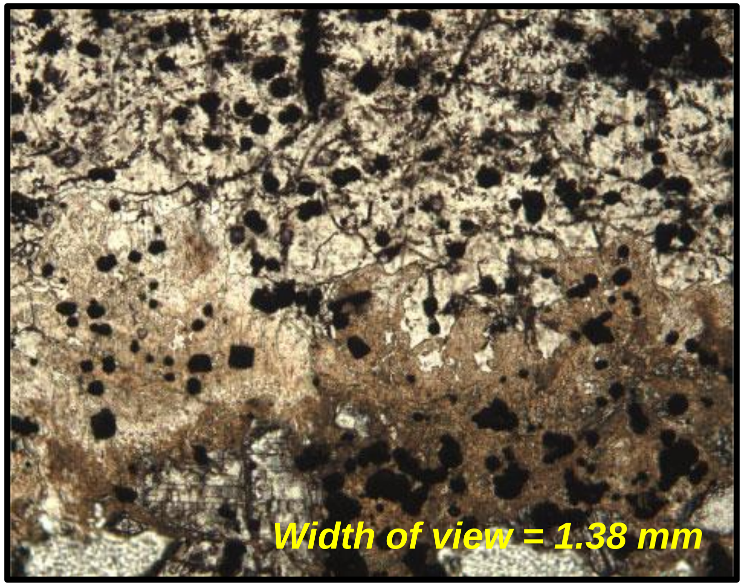

Metallic IP effects are negligible beyond 1 MHz

Introduction: Polarization

Interfacial polarization of clay particles – Membrane Polarization

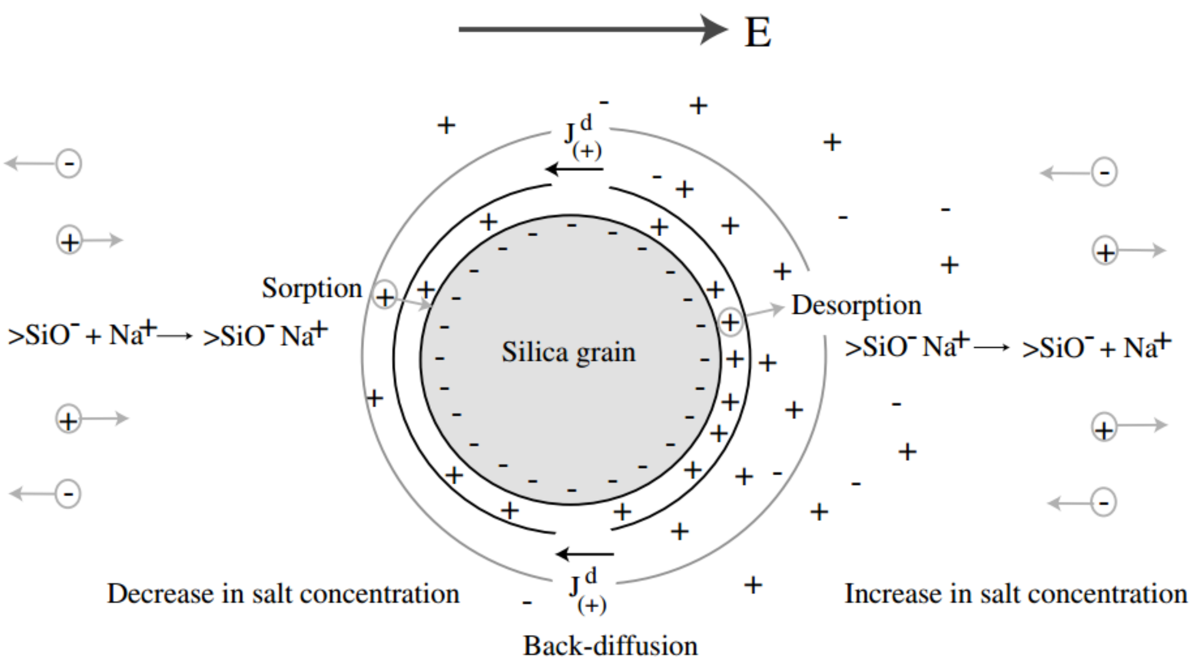

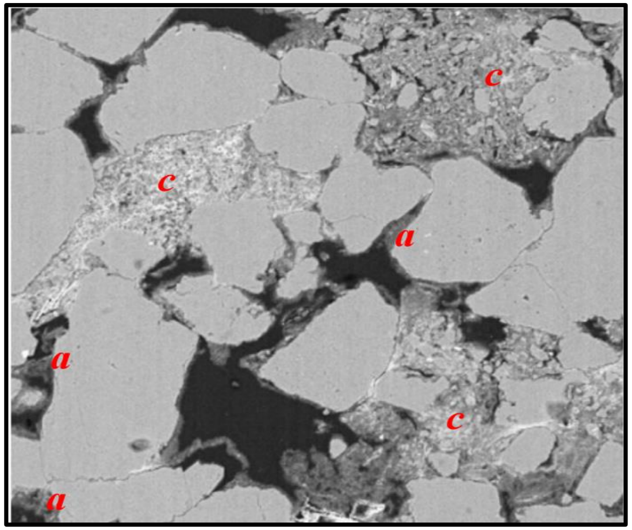

Revil et al., 2012

Membrane Polarization effects are negligible beyond 1 MHz

Motivation

Frequency dispersion in effective conductivity and permittivity

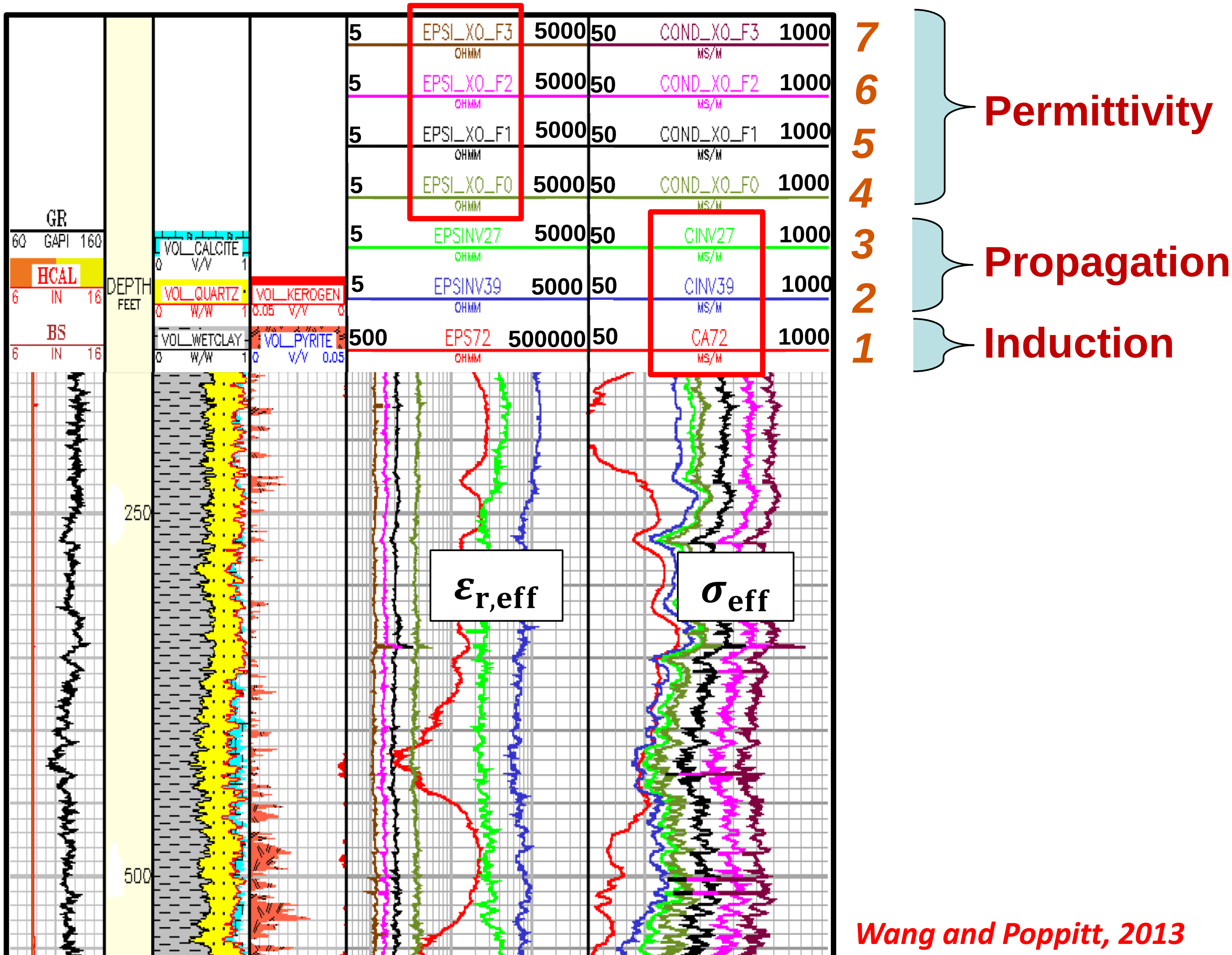

Wang and Poppitt, 2013

Motivation

Frequency dispersion in conductivity and permittivity

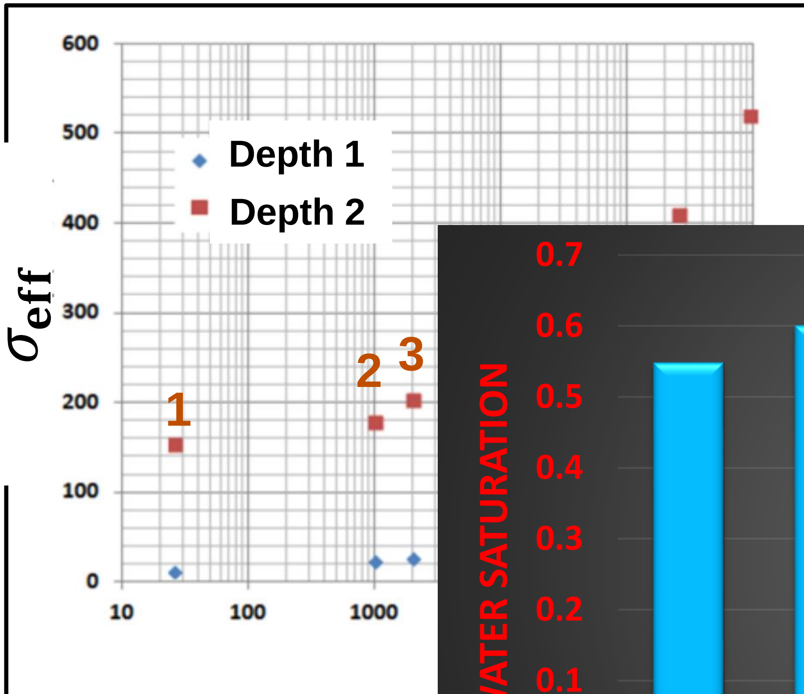

$$s_w = \frac{\left(\varepsilon^*_{r,eff}\right)^\alpha - (1-\phi)\left(\varepsilon^*_{r,m}\right)^\alpha - \phi\left(\varepsilon^*_{r,hy}\right)^\alpha}{\left(\varepsilon^*_{r,w}\right)^\alpha - \left(\varepsilon^*_{r,hy}\right)^\alpha}$$

CRIM Formula

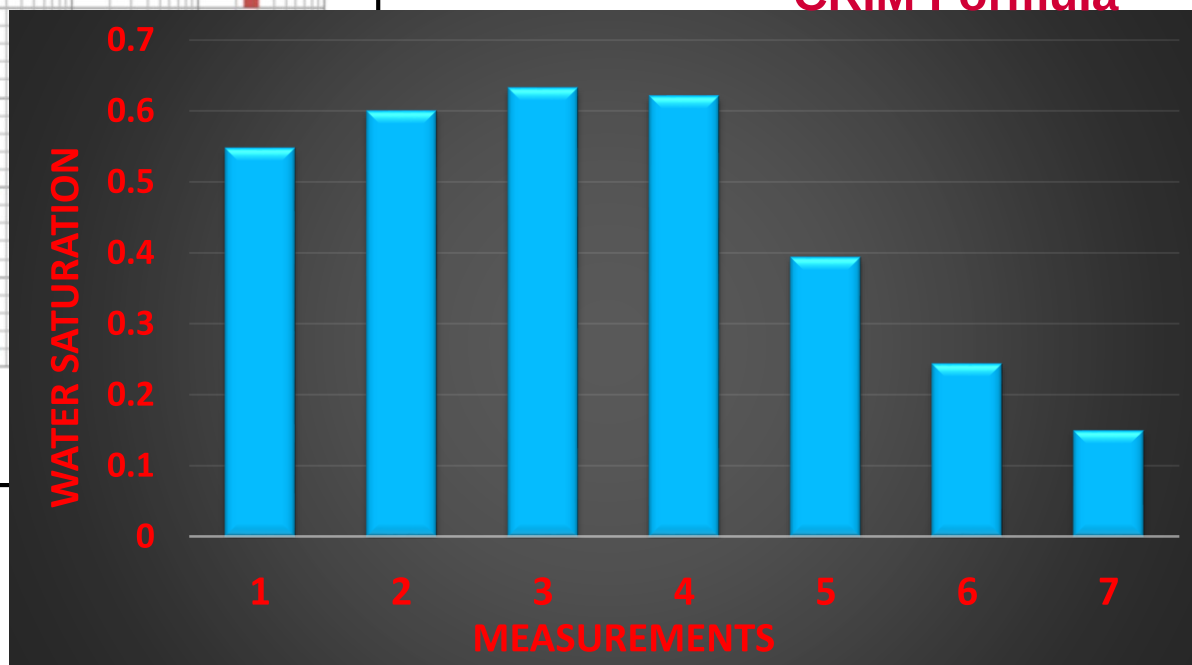

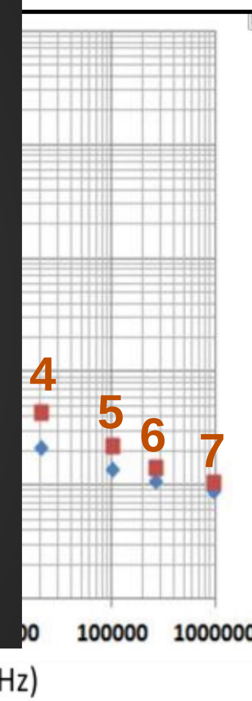

$$s_w = \sqrt[n]{\frac{\sigma_{eff}}{\sigma_w \phi^m}}$$

Archie's equation

Wang and Poppitt, 2013

Conductivity-Permittivity Interpretation

1 → **2** → **3**

1	2	3
Downhole EM Measurements	***EM Modeling and Inversion***	***Petrophysical estimation***
Voltage, Current, Phase, Amplitude	***Conductivity, Permittivity, Anisotropy, Azimuth, Dip***	***Water Saturation Brine conductivity Clay surface conductance***

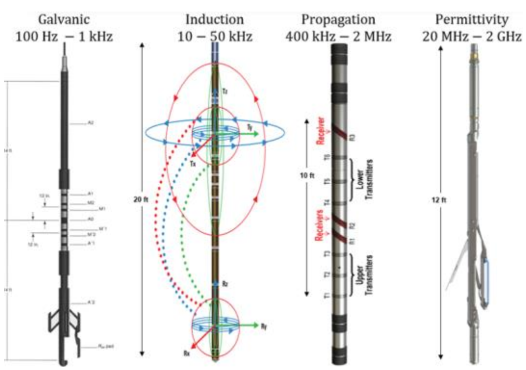

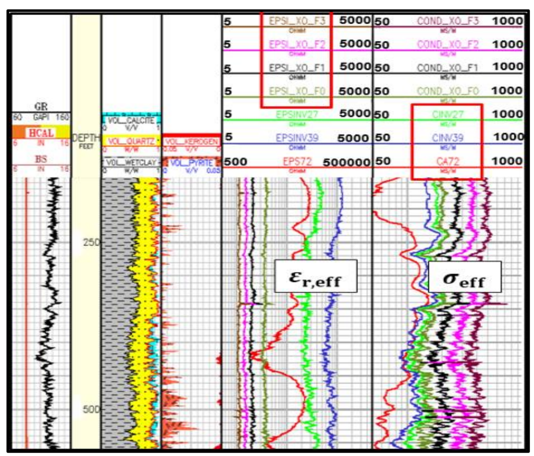

Archie's equation

$$s_w = \sqrt[n]{\frac{\sigma_{eff}}{\sigma_w \phi^m}}$$

CRIM

$$s_w = \frac{(\varepsilon^*_{r,eff})^\alpha - (1-\phi)(\varepsilon^*_{r,m})^\alpha - \phi(\varepsilon^*_{r,hy})^\alpha}{(\varepsilon^*_{r,w})^\alpha - (\varepsilon^*_{r,hy})^\alpha}$$

Conductivity-Permittivity Model

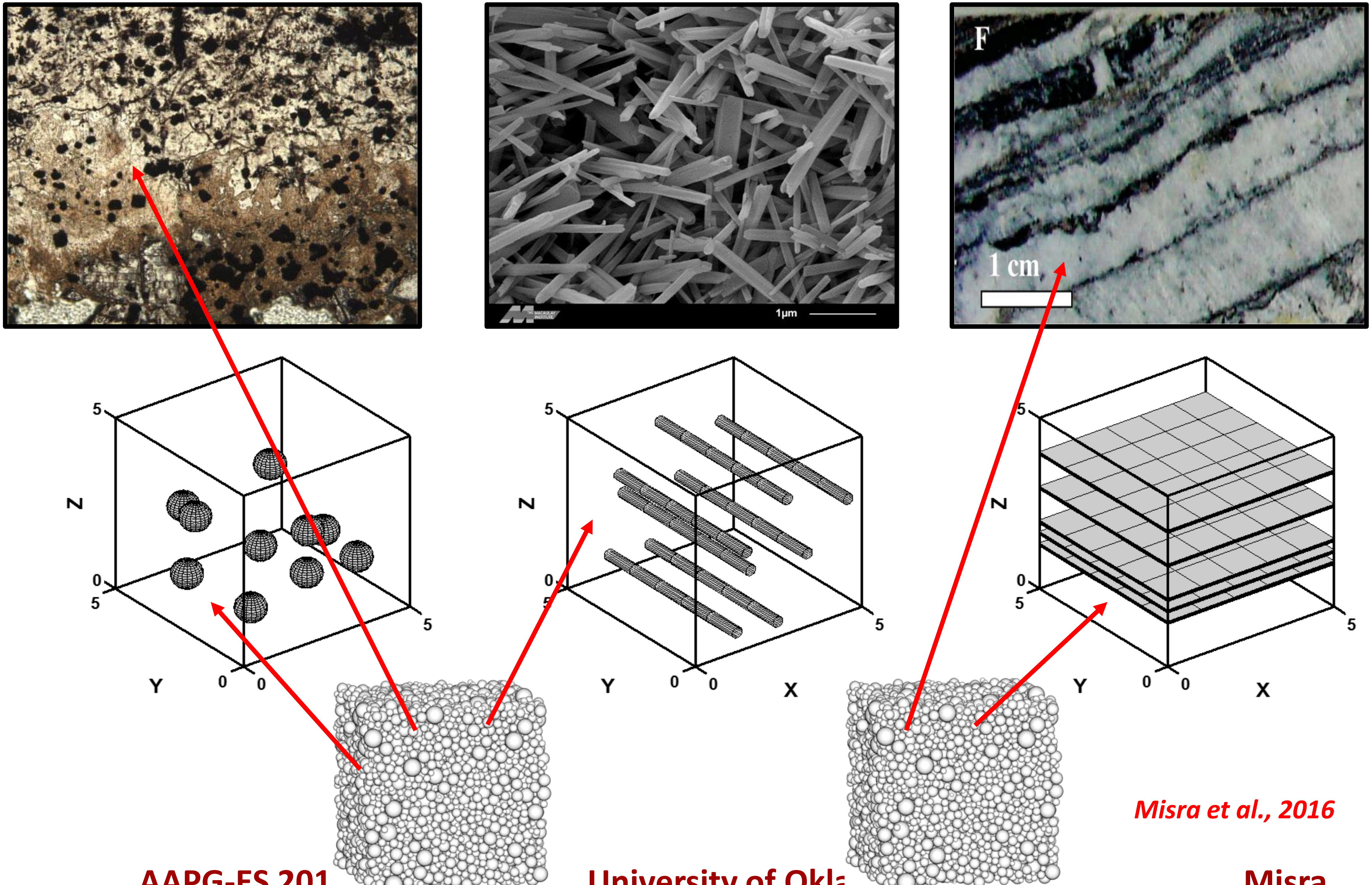

Misra et al., 2016

Conductivity-Permittivity Model

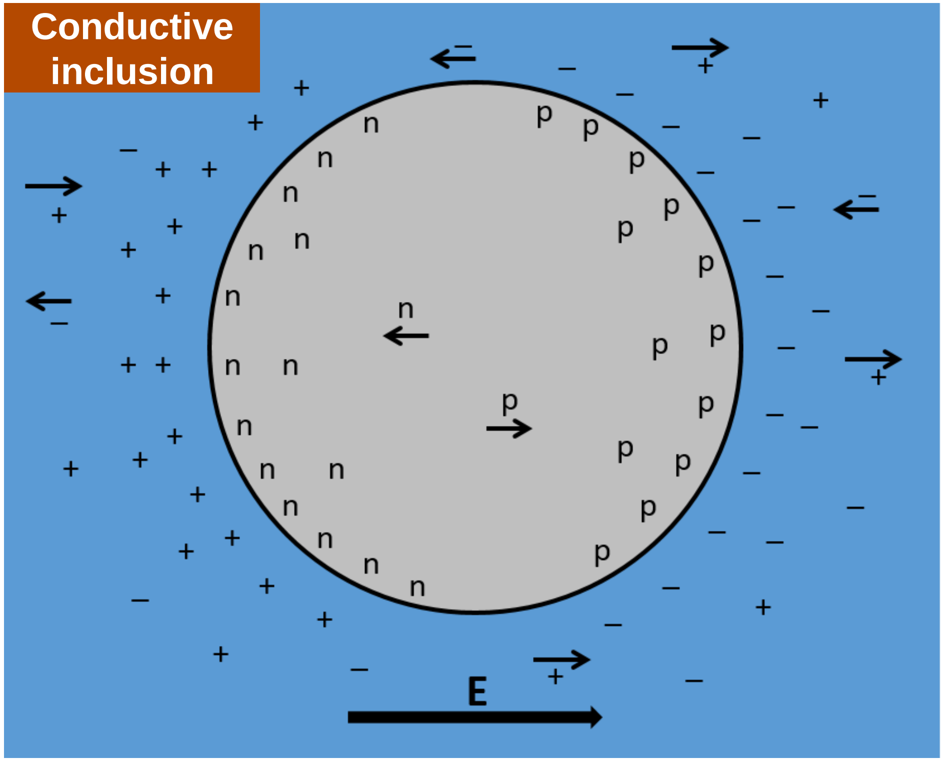

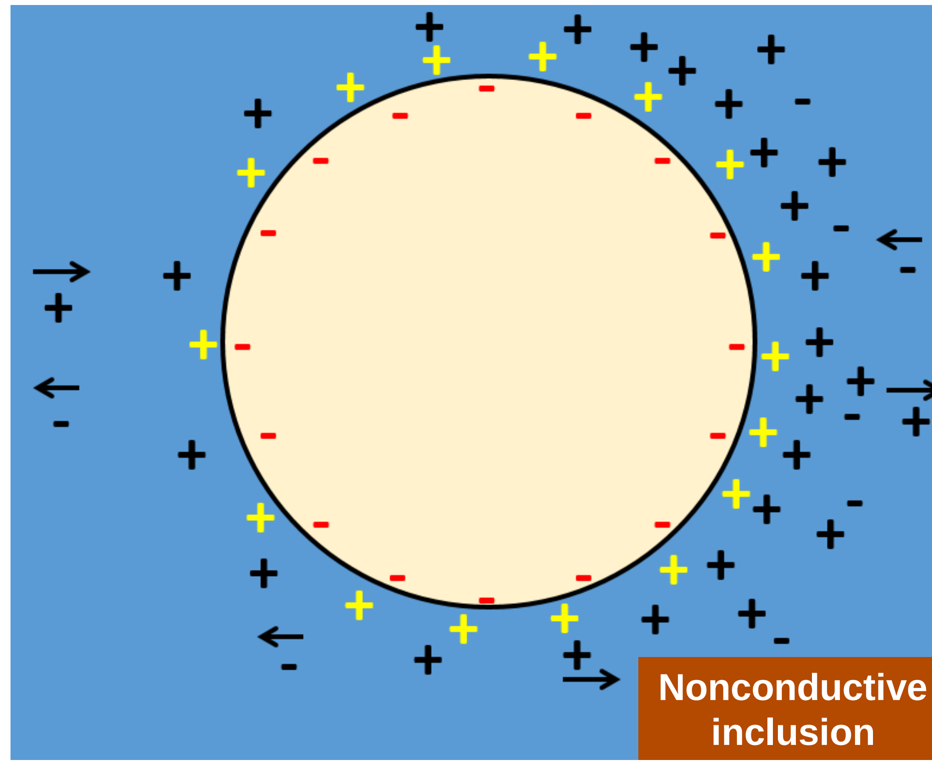

Misra et al., 2016

Conductivity-Permittivity Model

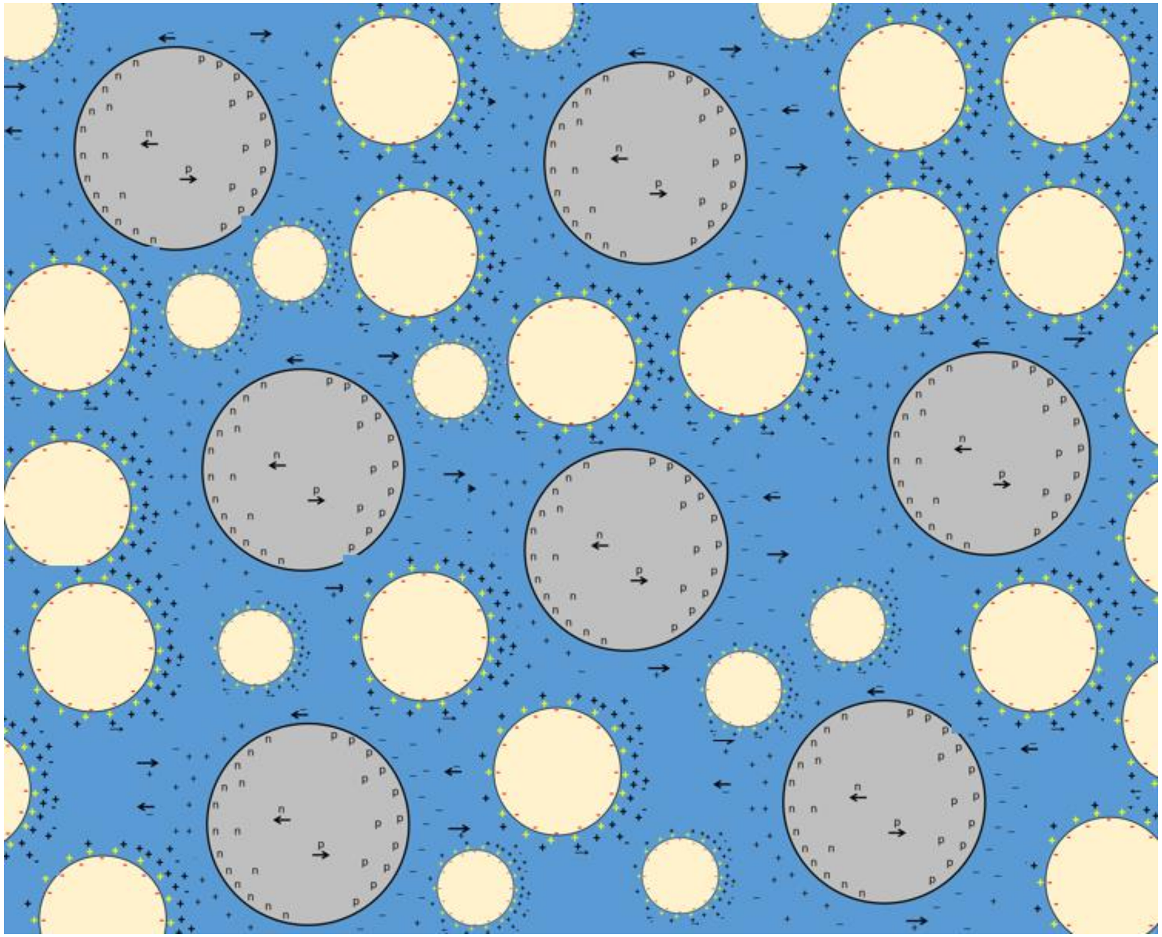

Misra et al., 2016

Alteration in electromigration

Account for charge accumulation and electrodiffusion

Conductivity-Permittivity Model

Input Parameters
Volume fraction of pyrite grains
Bulk conductivity of pyrite
Relative permittivity of pyrite
Diffusion coefficient of pyrite
Radius of pyrite grains
Volume fraction of clay
Relative permittivity of clay
Surface conductance of clay
Radius of spherical clay grains
Volume fraction of sand
Surface conductance of sand
Radius of sand grains
Bulk conductivity of brine
Relative permittivity of brine
Diffusion coefficient of brine
Relative permittivity of hydrocarbon
Water saturation

PS Model

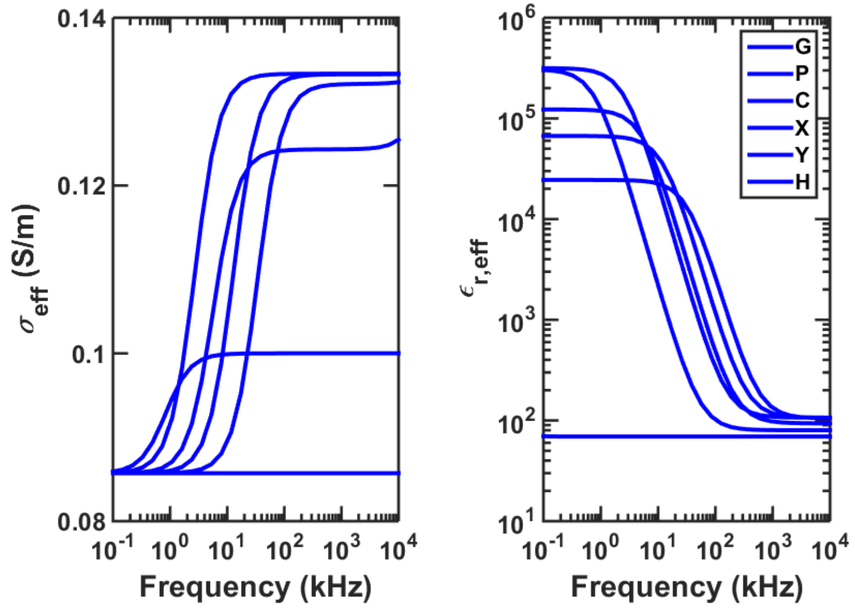

Model Predictions

Metallic Nature and Shape of Conductive Inclusions

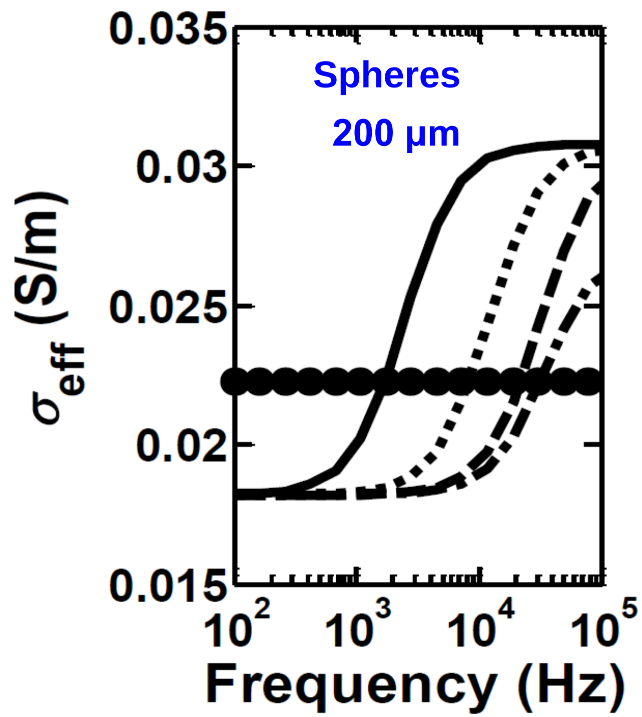

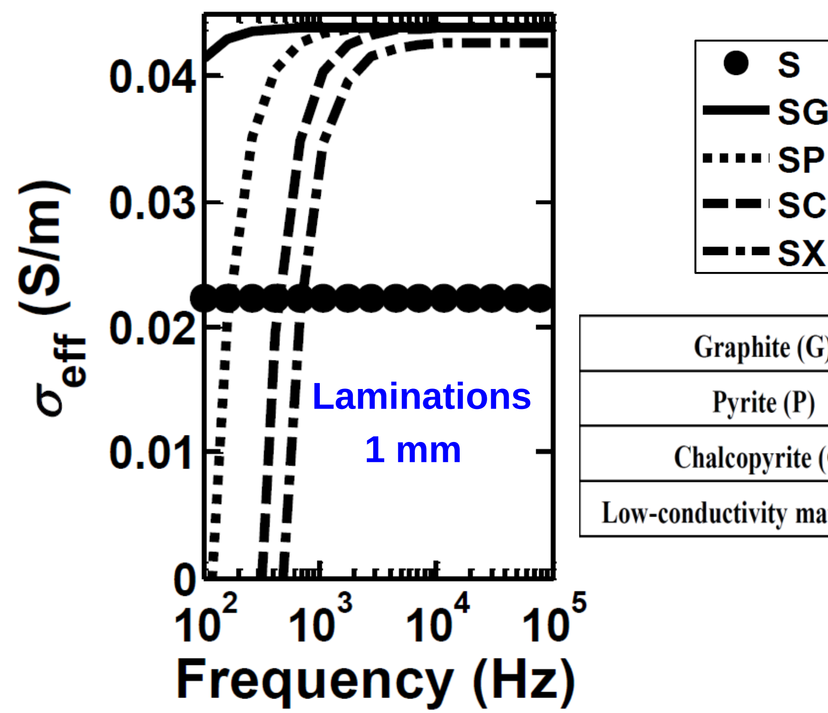

Graphite (G)
Pyrite (P)
Chalcopyrite (C)
Low-conductivity material (X)

Conductive Inclusions (5%)
+
Silica grains (70%)
+
Brine (0.1-S/m)

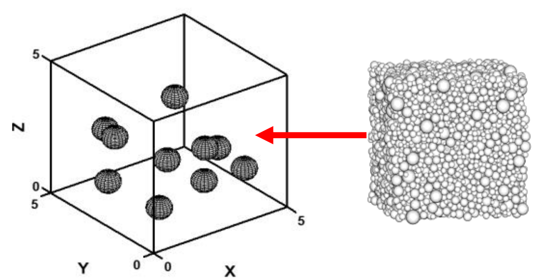

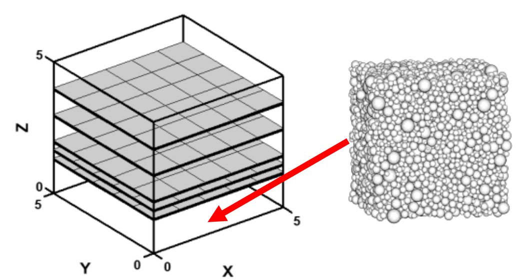

Model Predictions

Grain Size of Conductive Inclusions

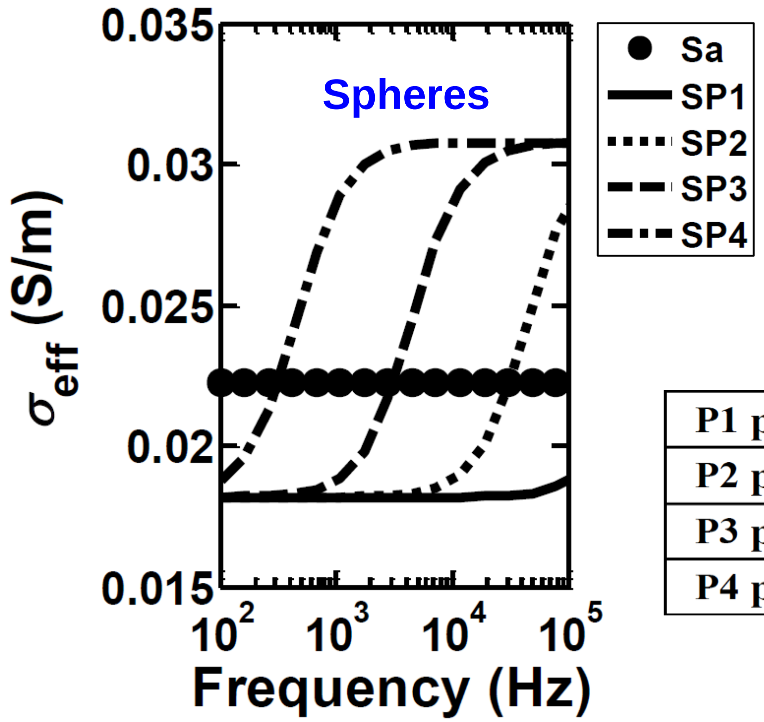

	Spherical inclusion	Sheet-like inclusion
P1 pyrite	2	200
P2 pyrite	20	600
P3 pyrite	200	1200
P4 pyrite	2000	2400

Conductive Inclusions (5%)
+
Silica grains (70%)
+
Brine (0.1-S/m)

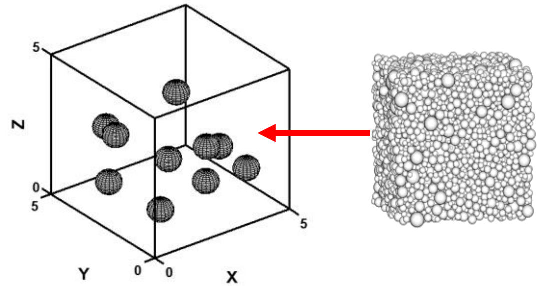

Model Predictions

Brine Conductivity and Conductive Inclusion Shape

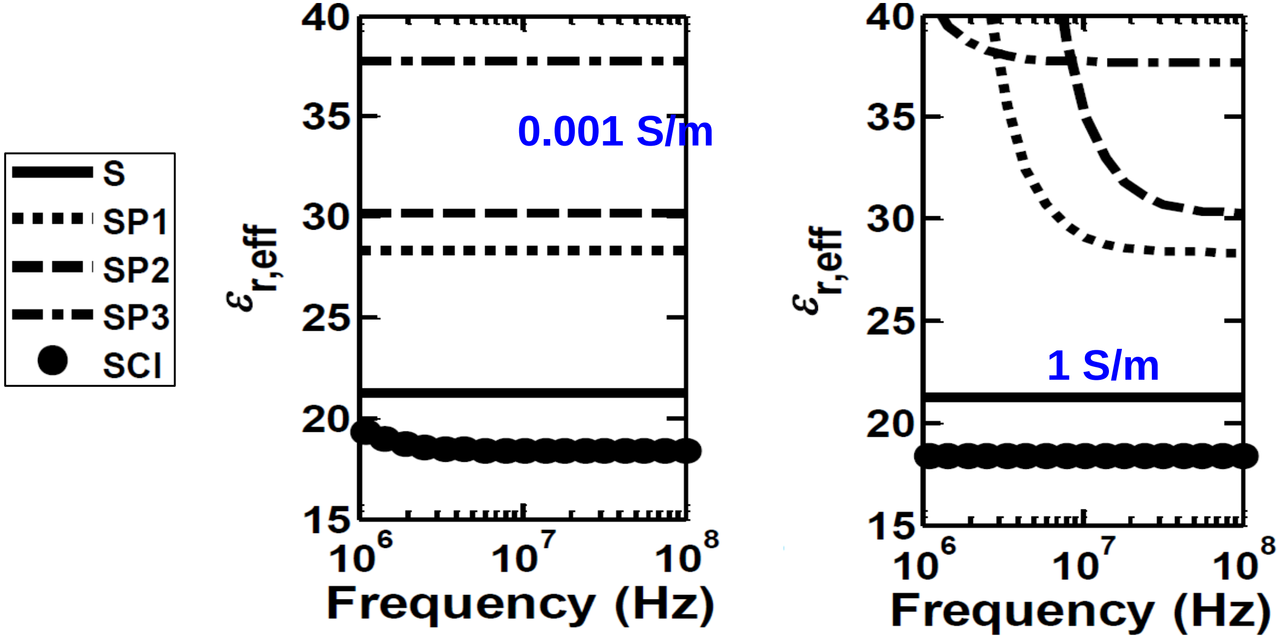

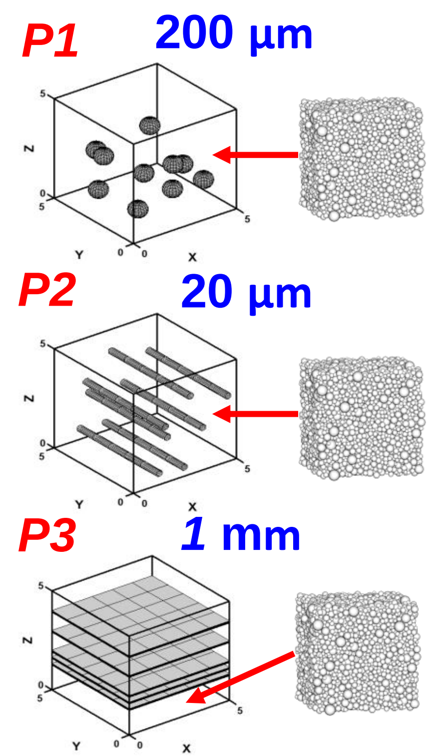

Conductive Inclusions (5%)
+
Silica grains (70%)
+
Brine (0.1-S/m)

Conductivity-Permittivity Inversion

Measurements

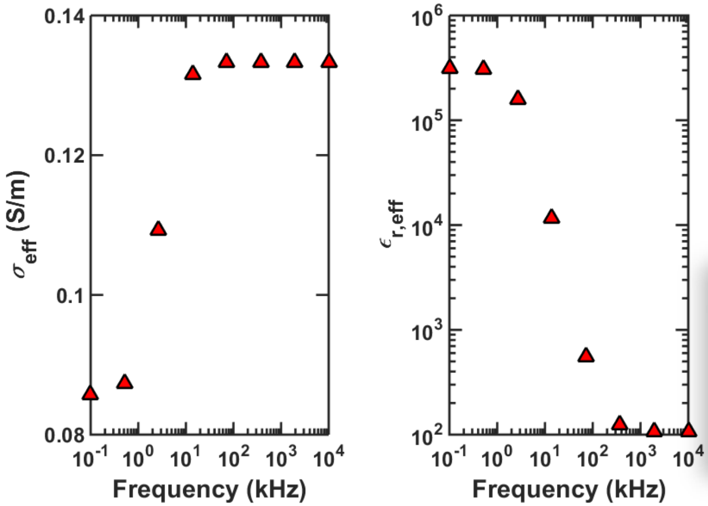

Model response

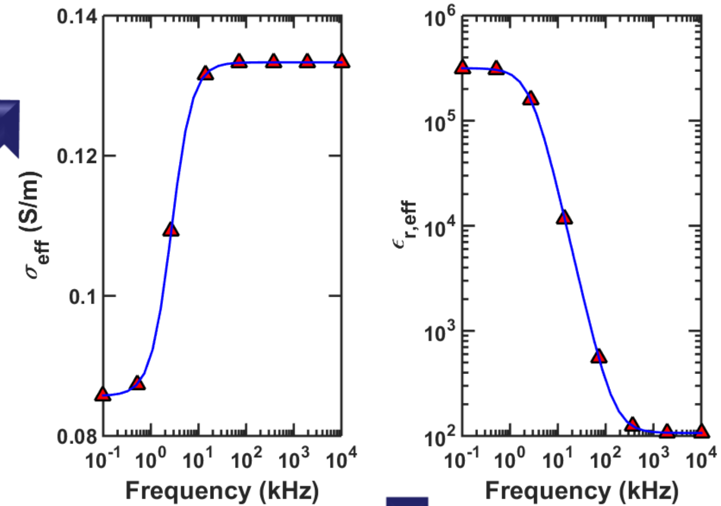

Conductivity-Permittivity Inversion

PS Model

Known Parameters	
Volume fraction of pyrite grains	Volume fraction of sand
Bulk conductivity of pyrite	Surface conductance of sand
Relative permittivity of pyrite	Radius of sand grains
Diffusion coefficient of pyrite	Relative permittivity of brine
Volume fraction of clay	Diffusion coefficient of brine
Relative permittivity of clay	Relative permittivity of hydrocarbon

Estimated Parameters
Water saturation
Bulk conductivity of brine
Surface conductance of clay
Radius of spherical clay grains
Radius of pyrite grains

Interpretation of Synthetic Data

Parameters	Unit	Parameter values for Synthetic Data 1	Parameter values for Synthetic Data 2
Volume fraction of pyrite grains	%	1	5
Bulk conductivity of pyrite	S/m	1000	1000
Relative permittivity of pyrite		30	30
Diffusion coefficient of pyrite	m^2/s	10^{-6}	10^{-6}
Radius of pyrite grains	μm	100	30
Volume fraction of clay	%	60	30
Relative permittivity of clay		5	5
Surface conductance of clay	S	10^{-6}	5×10^{-6}
Radius of spherical clay grains	μm	1	0.3
Volume fraction of sand	%	19	45
Surface conductance of sand	S	10^{-9}	10^{-9}
Radius of sand grains	μm	500	500
Bulk conductivity of brine	S/m	0.1	3
Relative permittivity of brine		80	80
Diffusion coefficient of brine	m^2/s	10^{-9}	10^{-9}
Relative permittivity of hydrocarbon		3	3
Water saturation	%	10	20

Interpretation of Synthetic Data

Synthetic Data 1

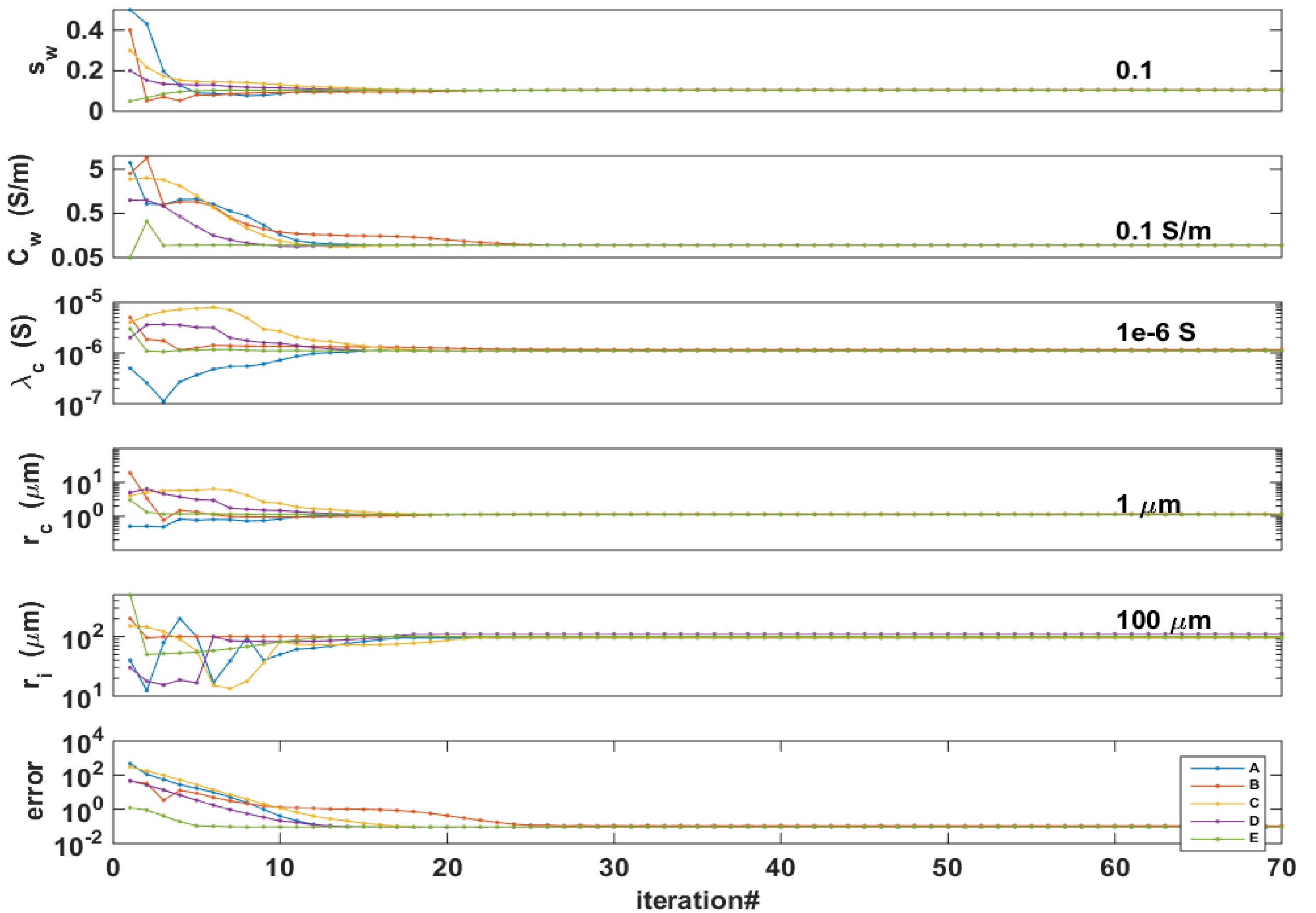

Interpretation of Synthetic Data

Synthetic Data 2

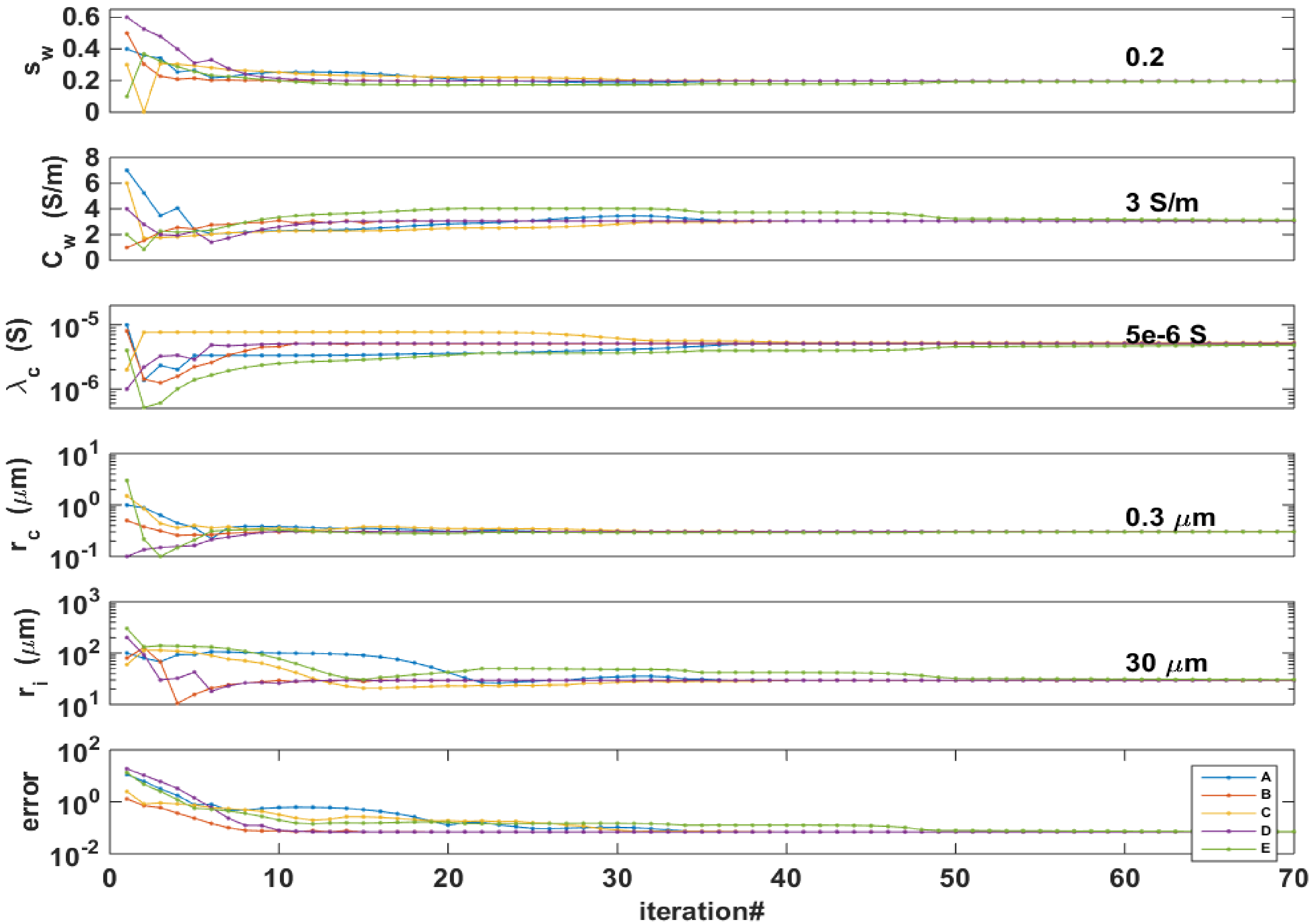

Interpretation of Synthetic Data

Synthetic Data 1

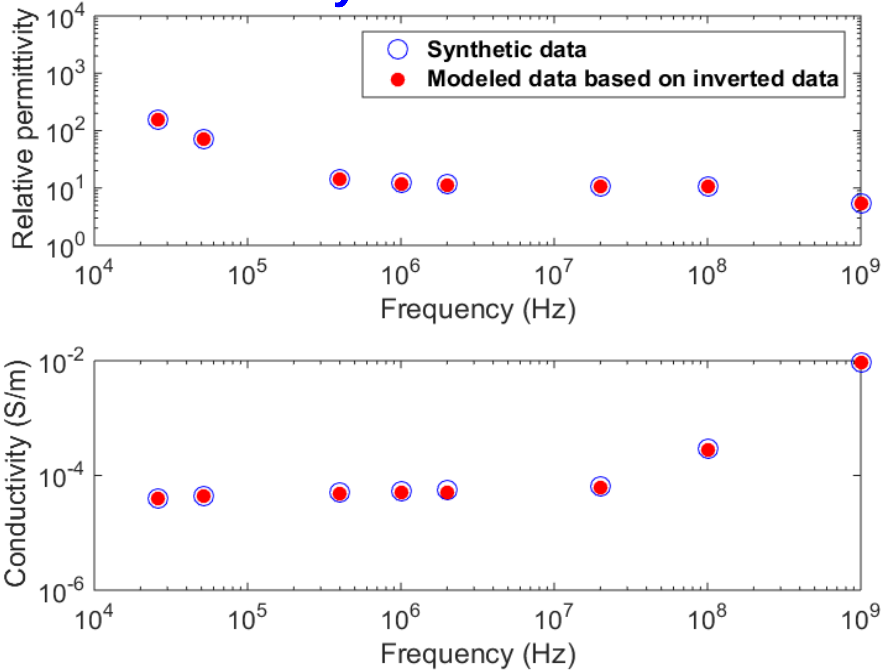

Synthetic Data 2

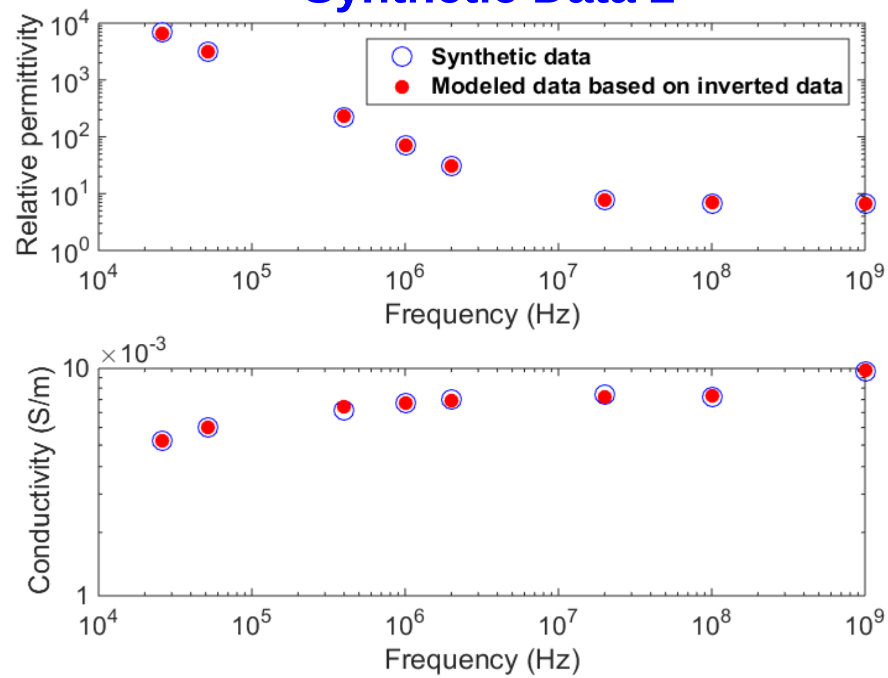

Interpretation of Subsurface Data

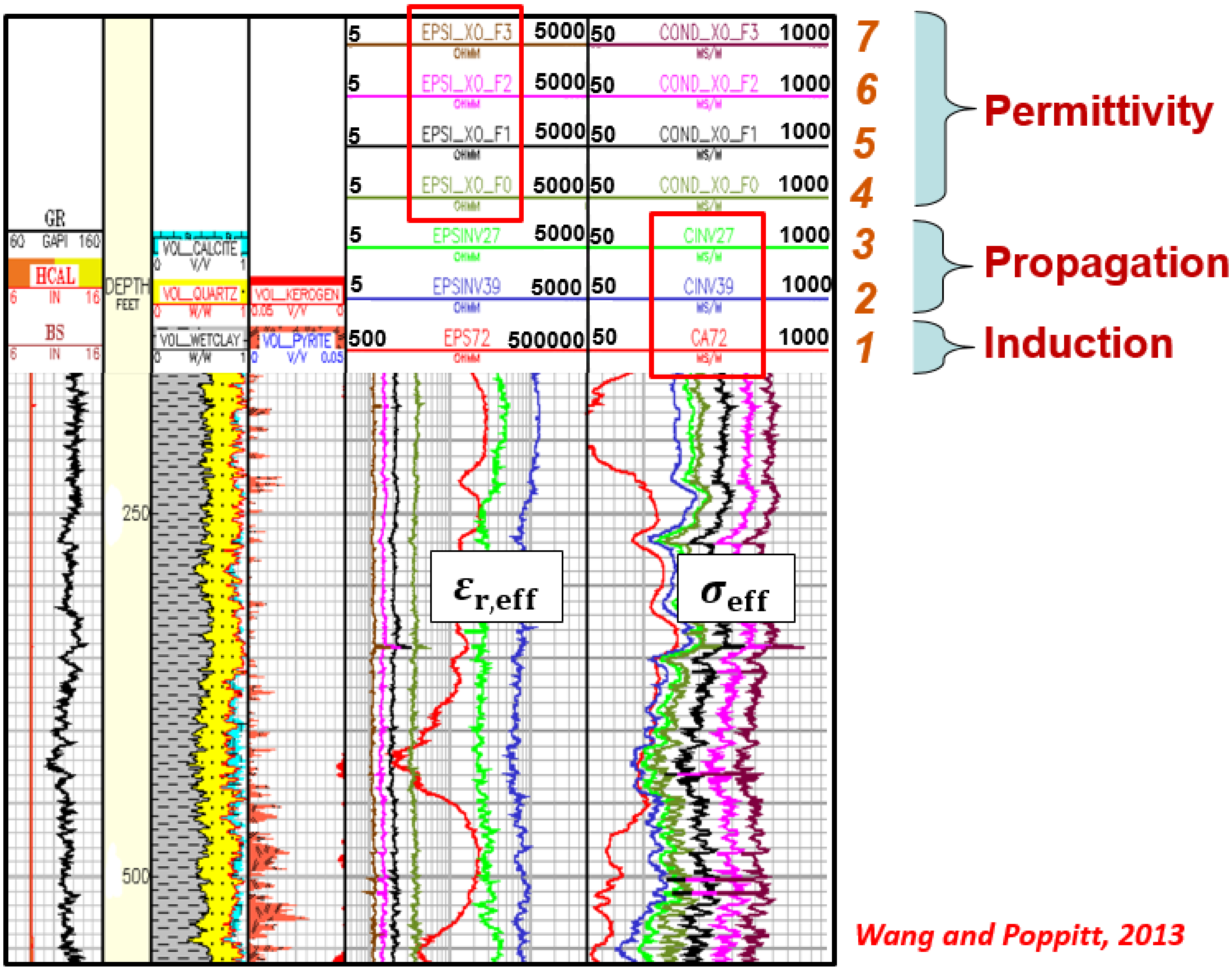

Wang and Poppitt, 2013

Interpretation of Subsurface Data

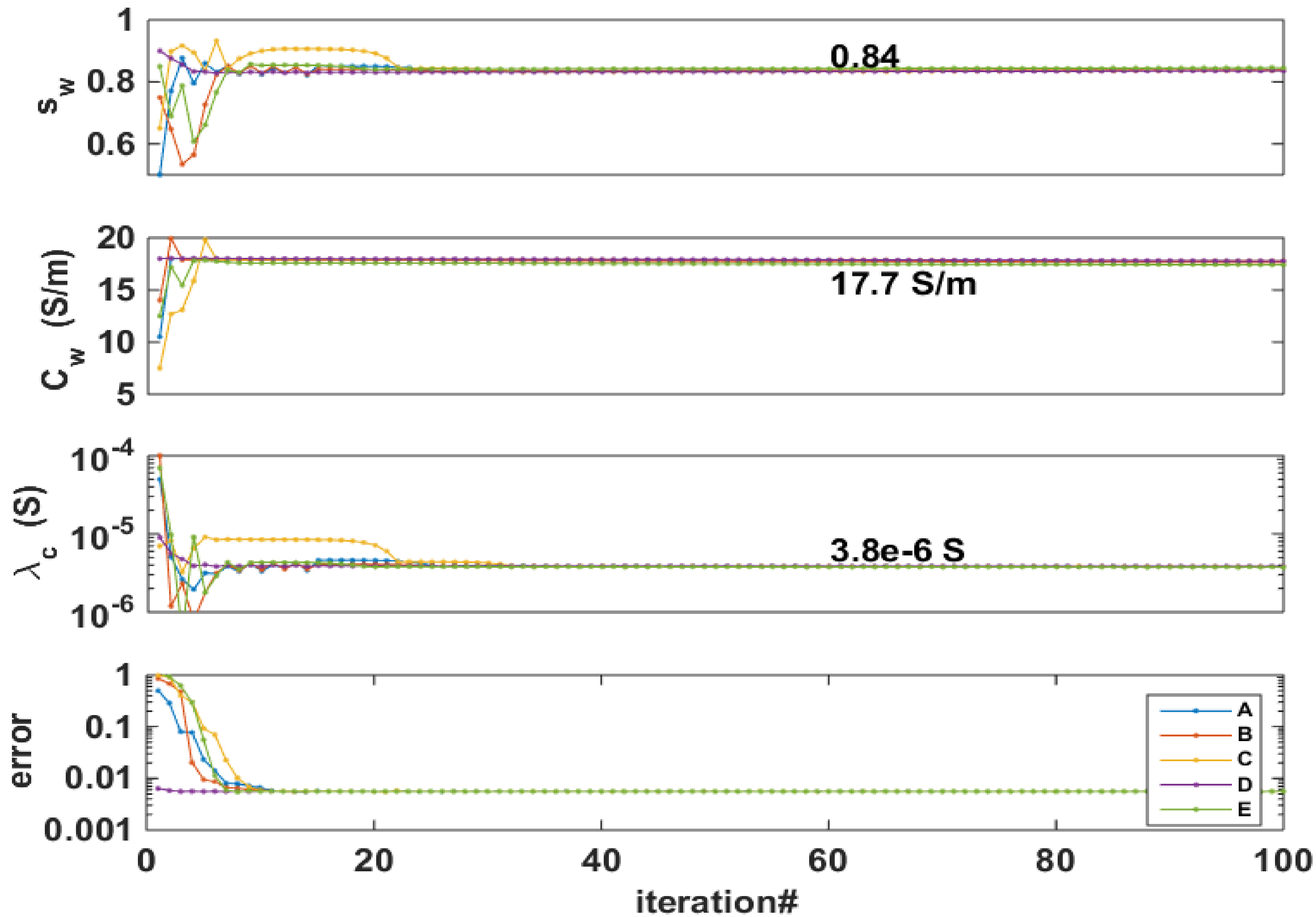

Interpretation of Subsurface Data

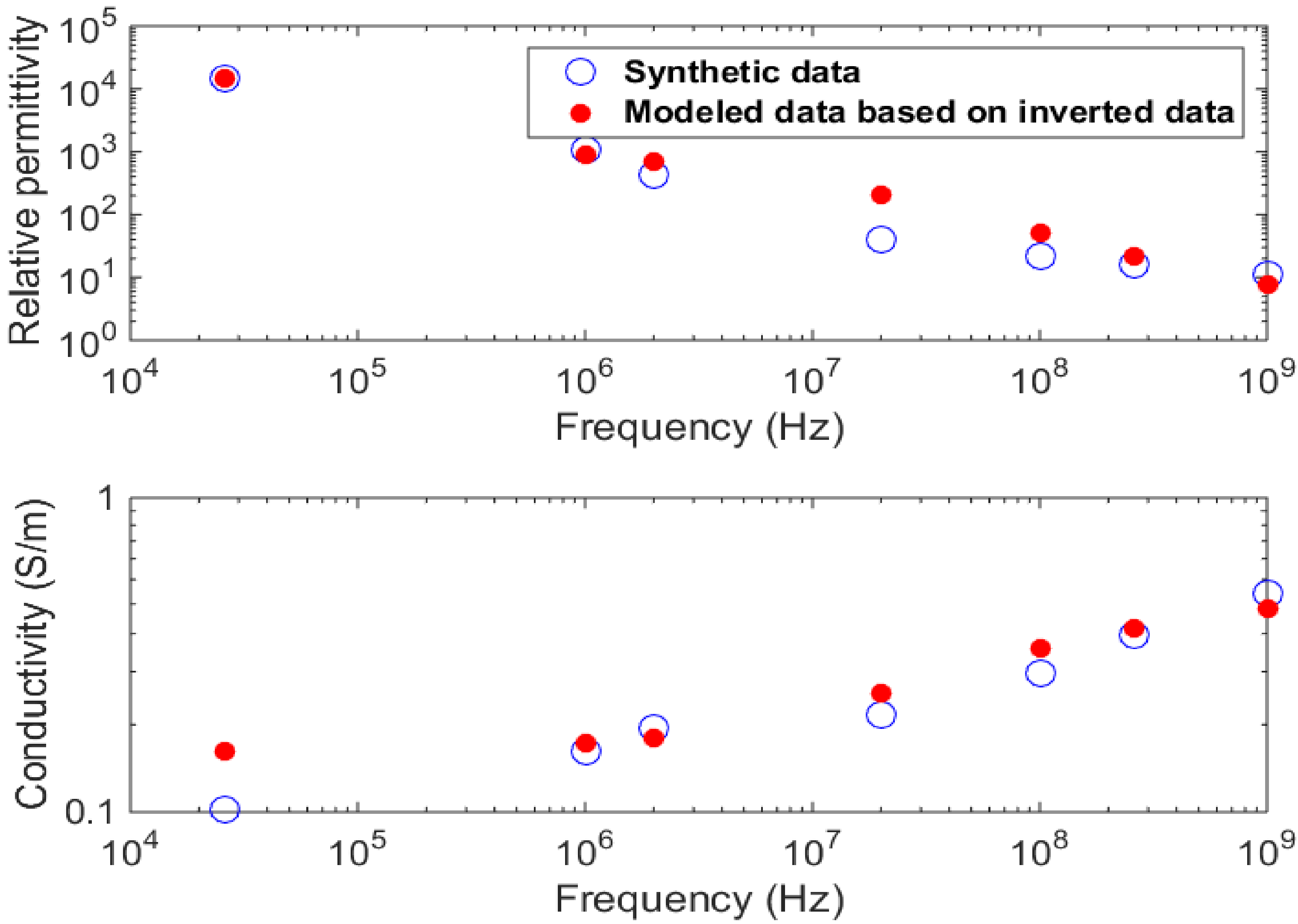

Conclusions

- Conductivity and permittivity of clay-bearing and conductive-mineral-bearing samples depend on:
  - Grain size of conductive inclusions
  - Metallic nature of conductive inclusions
  - Brine conductivity
  - Frequency of the applied EM field

- In contrast to EM induction and EM propagation measurements, galvanic resistivity measurements are:
  - Highly sensitive to laminations of clays and conductive minerals
  - Non-sensitive to disseminated spherical inclusions of clays and conductive minerals

- Dielectric dispersion measurements at operating frequencies higher than 100 MHz are unsusceptible to the effects of interfacial polarization of clays and pyrite grains.

Conclusions

- We developed an inversion scheme to jointly process the subsurface galvanic resistivity (< 1 kHz), EM induction (10 – 100 kHz), EM propagation (400 kHz – 10 MHz), and dielectric dispersion (10 MHz – 1 GHz) logs

- We presented a proof-of-concept exercise to assess water saturation, brine conductivity, surface conductance of clays, average grain size of clays, and average grain size of pyrite inclusions.

- The proposed joint inversion improves the accuracy of petrophysical interpretation of EM measurements by eliminating the effects of interfacial polarization of clays and pyrite inclusions.

Thank You